Chapter 20
The EMEP/MSC-E Mercury Modeling System

Oleg Travnikov and Ilia Ilyin

Summary The EMEP/MSC-E hemispheric chemical transport model (MSCE-HM-Hem) and its regional version (MSCE-HM) are applied for operational calculations of mercury transboundary pollution within the European region and in the Northern Hemisphere. This chapter contains examples of the models application for assessment of mercury atmospheric dispersion and deposition both on hemispheric and regional scales. Model simulations of mercury atmospheric dispersion in the Northern Hemisphere have been performed for the period 1990-2004. Long-term changes of mercury deposition during this period have been evaluated for different continents and regions of the Northern Hemisphere. Obtained modelling results have been compared with long-term monitoring data from various national and international networks. Besides, intercontinental transport of mercury as well as sensitivity of mercury deposition in the Northern Hemisphere to emission reduction in different continents have been estimated.

20.1 Introduction

Mercury is among the priority pollutants considered under the Convention on Long-Range Transboundary Air Pollution (CLRTAP). Along with other heavy metals it was included into the Protocol on Heavy Metals – an international binding instrument under the Convention regulating atmospheric emissions of these pollutants and aimed at reduction of their adverse effects on human health and the environment. Scientific support of development and implementation of the Protocol is provided by the Cooperative Programme for Monitoring and Evaluation of the Long-range Transmission of Air Pollutants in Europe (EMEP). To meet requirements of the Protocol the Meteorological Synthesizing Centre - East of EMEP (EMEP/MSC-E) develops and applies appropriate chemical transport models to provide Parties to the Convention with information on transboundary fluxes and deposition of heavy metals in Europe including mercury.

This chapter contains examples of application of the EMEP/MSC-E chemical transport models for assessment of mercury atmospheric dispersion and deposition

N. Pirrone and R. Mason (eds.), *Mercury Fate and Transport in the Global Atmosphere*,
DOI: 10.1007/978-0-387-93958-2_20,

both on hemispheric and regional scales. Particular attention is paid to evaluation of long-term changes of mercury deposition in different parts of the Northern Hemisphere and to estimates of relative importance of the intercontinental atmospheric transport for mercury deposition and their sensitivity to emission reduction in various continents.

20.2 Model Description

The EMEP/MSC-E hemispheric chemical transport model (MSCE-HM-Hem) and its regional version (MSCE-HM) are applied for operational calculations of mercury and other heavy metals transboundary pollution within the European region and in the Northern Hemisphere in connection with the EMEP programme and other activities relating to the CLRTAP. Detailed description of the models is available in (Travnikov and Ryaboshapko, 2002; Travnikov and Iliyn, 2005; Travnikov, 2005). A brief overview of the model formulation is presented below.

The hemispheric MSCE-HM-Hem model is a three-dimensional Eulerian type chemical transport model driven by off-line meteorological data. The model domain covers the whole Northern Hemisphere with resolution 2.5° × 2.5° (Figure 20.1(a)). The terrain-following pressure-based vertical coordinate consists of eight irregular layers up to the lower stratosphere. The model considers mercury emissions from anthropogenic and natural sources, transport in the atmosphere, chemical transformations both in gaseous and aqueous phases, and deposition to the ground. The regional version of the model (MSCE-HM) is formulated on the polar stereographic projection and covers the European region and surrounding areas by a regular grid with 50×50 km spatial resolution at 60°N (Figure 20.1b). Both models have the same formulation of major physical and chemical processes and are coupled by the one-way nesting. Daily mean concentrations of three atmospheric mercury forms (Hg^0, $Hg^{(II)}_{gas}$, Hg_{part}) pre-calculated with the hemispheric model are used for definition of initial and boundary conditions for the regional model.

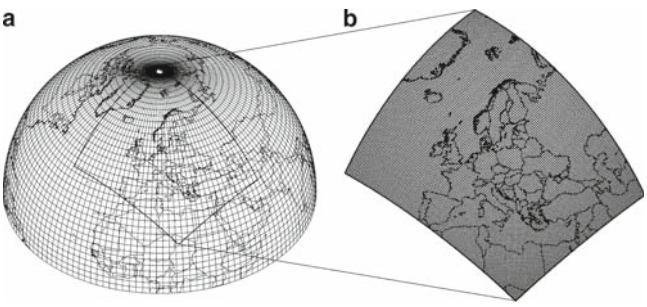

Figure 20.1 Hemispheric (**a**) and the EMEP regional (**b**) grids of the MSCE-HM-Hem and MSCE-HM models

The chemical scheme of mercury transformation in the atmosphere is based on the kinetic mechanism developed by Petersen et al. (1998). The original scheme was optimized in order to accelerate the model performance for operational calculations. For this purpose very slow reactions were neglected, whereas very fast ones were replaced by appropriate equilibriums. The model description of physical and chemical transformations of mercury in the atmosphere includes dissolution in cloud droplets, gas-phase and aqueous-phase oxidation by ozone, chlorine and hydroxyl radical, aqueous-phase reduction via decomposition of sulphite complexes, formation of chloride complexes, and adsorption by soot particles in cloud water. A summary of all chemical transformations included to the model is presented in Table 20.1.

The monthly mean data on air concentration of chemical reactants involved in reactions with mercury are taken from Wang et al. (1998) for ozone, Chin et al. (1996) for sulphur dioxide, and Spivakovsky et al. (2000) for hydroxyl radical. The original data were interpolated to the model grid. In order to take into account the diurnal cycle of OH radical we assume zero concentration at night and concentrations proportional to the cosine of the solar zenith angle during daytime. Besides, air concentrations of OH were decreased by a factor of 2 in the cloud environment and below clouds to account for reduction of photochemical activity (Seigneur et al., 2001). Besides, following Seigneur et al. (2001) we adopt air concentration of molecular chlorine in the lowest model layer over the ocean to be 100 ppt at night and 10 ppt during daytime and zero concentration over land. Model description of removal processes includes dry deposition and wet scavenging. The dry deposition scheme is based on the resistance analogy approach (Wesely and Hicks, 2000) and allows taking into account deposition to different land cover types (forests, grassland, water surface etc.). Dry deposition of particles to vegetation is described using the theoretical formulation by Slinn (1982) and fitted to experimental data (Ruijgrok et al., 1997; Wesely et al., 1985).

The parameterization of dry deposition to water surfaces is based on the approach suggested by Williams (1982) taking into account the effects of wave breaking and aerosol washout by seawater spray. Parameters of dry deposition of gaseous oxidised mercury are chosen as for those of nitric acid (zero surface resistance) because of similar solubility of these substances. Besides, dry deposition of gaseous elemental mercury to vegetation is considered. The deposition velocity of this form varies from 0 to 0.03 cm s^{-1} depending on surface temperature, solar radiation and vegetation type. The model distinguishes in-cloud and sub-cloud wet scavenging of particulate species and highly soluble reactive gaseous mercury based on empirical data. Besides, the precipitation rate is scaled for convective precipitation according to Walton et al. (1988) to take into account fractional coverage of a grid cell with precipitating clouds.

The hemispheric MSCE-HM-Hem model is driven by off-line meteorological parameters supplied by the low atmosphere diagnostics system (SDA) developed in co-operation with Hydro-meteorological Centre of Russia (Rubinstein and Kiktev, 2000). The system provides 6-hour weather prediction data along with estimates of the atmospheric boundary layer parameters and covers the Northern Hemisphere with the model spatial resolution. NCAR/NCEP re-analysis data is utilized as the

Table 20.1 Summary of mercury transformations included into the model

Reactions and equilibriums	k or H	Units	Reference
$Hg^0_{(gas)} + O_3(gas) \rightarrow Hg(II)_{(part)} + products$	2.1×10^{-18} exp(-1247/T)	cm^3 $molecule^{-1}$ s^{-1}	Hall, 1995
$Hg^0_{(gas)} + {}^{\bullet}OH_{(gas)} \rightarrow Hg(II)_{(part)} + products$	8.7×10^{-14}	cm^3 $molecule^{-1}$ s^{-1}	Sommar et al., 2001
$Hg^0_{(gas)} + Cl_2(gas) \rightarrow Hg(II)_{(gas)}$	2.6×10^{-18}	cm^3 $molecule^{-1}$ s^{-1}	Ariya et al., 2002
$Hg^0_{(aq)} + O_3(aq) \rightarrow Hg^{2+}_{(aq)} + products$	4.7×10^{7}	$M^{-1}s^{-1}$	Munthe, 1992
$Hg^0_{(aq)} + {}^{\bullet}OH_{(aq)} \rightarrow Hg^{2+}_{(aq)} + products$	2.4×10^{9}	$M^{-1}s^{-1}$	Gårdfeldt et al., 2001
$Hg^0_{(aq)} + Cl(l)_{(aq)} \rightarrow Hg^{2+}_{(aq)} + products$	2×10^{6}	$M^{-1}s^{-1}$	Lin and Pehkonen, 1999
$Hg^{2+}_{(aq)} + 2SO^{2-}_{3(aq)} \rightarrow Hg(SO_3)^{2+}_{(aq)}$	$1.1\times10^{-21}[SO_{2(gas)}]$ $^{2}\times10^{4pH}$ *	s^{-1}	Petersen et al., 1998
$Hg(SO_3)^{2-}_{2(aq)} \rightarrow {}_qHg^0_{(aq)} + products$	4.4×10^{-4}	s^{-1}	Petersen et al., 1998
$Hg_nCl_{m(dis)} \leftrightarrow Hg^{2+}_{(aq)}$	f($[Cl^-]$) **	1	Lurie, 1971
$Hg_nCl_{m(dis)} \leftrightarrow Hg_nCl_{m(soot)}$	0.2	1	Petersen et al., 1998
$Hg(SO_3)^{2-}_{2(dis)} \leftrightarrow Hg(SO_3)^{2-}_{2\ (soot)}$	0.2	1	Petersen et al., 1998
$Hg^0_{(gas)} \leftrightarrow Hg^0_{(aq)}$	1.76×10^{-23}T exp(9.08(T_0/T-1))	M cm^3 $molecule^{-1}$	Andersson et al., 2004
$HgCl_{2(gas)} \leftrightarrow HgCl_{2(aq)}$	1.75×10^{-16}T exp(18.75(T_0/T-1))	M cm^3 $molecule^{-1}$	Ryaboshapko et al., 2001
$O_{3(gas)} \leftrightarrow O_{3(aq)}$	1.58×10^{-24}T exp(7.8(T_0/T-1))	M cm^3 $molecule^{-1}$	Sander, 1997
${}^{\bullet}OH_{(gas)} \leftrightarrow {}^{\bullet}OH_{(aq)}$	3.41×10^{-21}T exp(17.72(T_0/T-1))	M cm^3 $molecule^{-1}$	Jacobson, 1999
$Cl_{2(gas)} \leftrightarrow Cl(l)_{(aq)}$	4.48×10^{-16}	M cm^3 $molecule^{-1}$	Lin and Pehkonen, 1999

* $[SO_{2(gas)}]$ is in ppbv

** $$\frac{[Hg_nCl_{m(dis)}]}{[Hg^{2+}_{(aq)}]} = \frac{[Cl^-_{(aq)}]}{1.82\cdot10^{-7}} + \frac{[Cl^-_{(aq)}]^2}{6.03\cdot10^{-14}} + \frac{[Cl^-_{(aq)}]^3}{8.51\cdot10^{-15}} + \frac{[Cl^-_{(aq)}]^4}{8.51\cdot10^{-16}}$$

input information for the system. The regional MSCE-HM model is driven by meteorological data pre-processed by the MM5 - Fifth Generation Penn State/NCAR Mesoscale Model (Grell et al., 1995). The pre-processor utilizes the NCAR/NCEP re-analysis or ECMWF data as the input information and provides 6-hour weather prediction data with the same spatial resolution as that of the transport model.

Anthropogenic emissions data for long-term calculations during the period 1990-2005 were prepared utilizing global mercury emission datasets available for the years 1990, 1995, and 2000 (CGEIC website; Pacyna et al., 2003; Pacyna et al., 2006). For other years of the period the linear interpolation was applied, except for emissions for years 2001-2004 which were taken equal to those in 2000 because of absence of more recent data. However, this assumption evidently does not allow taking into account significant growth of mercury emissions in China since 2000 (see Chapters 2 and 3). Estimated long-term changes of total mercury anthropogenic emissions in the Northern Hemisphere and their spatial distribution in 2000 are presented in Figure 20.2.

As seen, relative contribution of European and North American sources to total hemispheric emission significantly decreased in the first half of the period while the contribution of Asian sources increased. Thus, the overall emission changed slightly between 1990 and 2004.

Natural emission and re-emission of mercury from soil and seawater was taken into account using global estimates by Lamborg et al. (2002). Spatially resolved emission flux was obtained by distribution of the global emission values over Earth's surface depending on the soil temperature for emissions from land and proportional to the primary production of organic carbon for emissions from the oceans (Travnikov and Ryaboshapko, 2002). It was expected that mercury is emitted from natural surfaces in elemental gaseous form. The temperature dependence of soil emission was described by an Arrhenius type equation with empirically derived activation energy about 20 kcal mol^{-1} (Kim et al., 1995; Carpi and Lindberg, 1998;

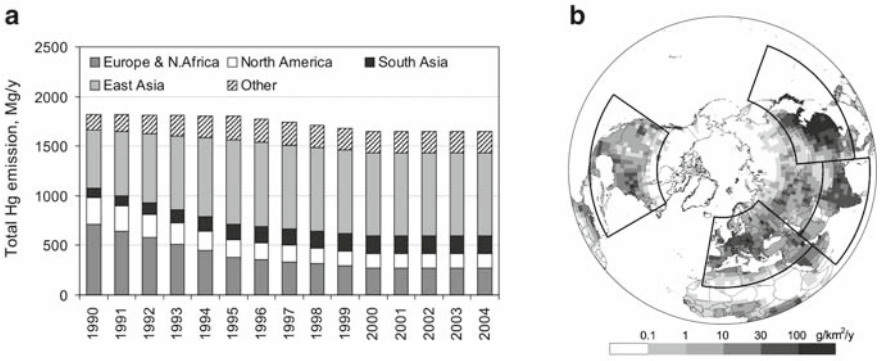

Figure 20.2 Long-term changes of mercury anthropogenic emissions in the Northern Hemisphere (**a**) and spatial distribution of Hg anthropogenic emissions in 2000 (**b**). Solid lines depict source regions selected for the analysis

Poissant and Casimir, 1998; Zhang et al., 2001). Evasion of Hg from geochemical mercuriferrous belts (Gustin et al., 1999) was assumed to be 10 times higher then that from background soils. Monthly mean satellite based data on the ocean primary production of carbon (Behrenfeld and Falkowski, 1997) were utilized to distribute the natural mercury emission flux over the ocean.

Two-years model spin-up was performed to fill up the atmosphere with mercury. To take into account the inter-hemispheric transport of mercury a fixed gradient of elemental mercury concentration of 0.05 ng m^{-3} degree was set at the equator. This value was obtained from approximation of measurement data from the ocean cruises (Slemr, 1996).

20.3 Results and Discussion

Model simulations of mercury atmospheric dispersion in the Northern Hemisphere were performed for the period 1990-2004. Long-term changes of mercury deposition during this period were evaluated for different continents and regions of the Northern Hemisphere. Obtained modelling results were compared with long-term monitoring data from various national and international networks (EMEP, NADP/MDN, CAMnet etc.) Besides, intercontinental transport of mercury as well as sensitivity of mercury deposition in the Northern Hemisphere to emission reduction in different continents were estimated. Major modelling results are discussed below.

20.3.1 Spatial distribution and long-term trends

Spatial patterns of total mercury deposition in the Northern Hemisphere and, with higher resolution, in Europe are illustrated in Figure 20.3 for the year 2001.

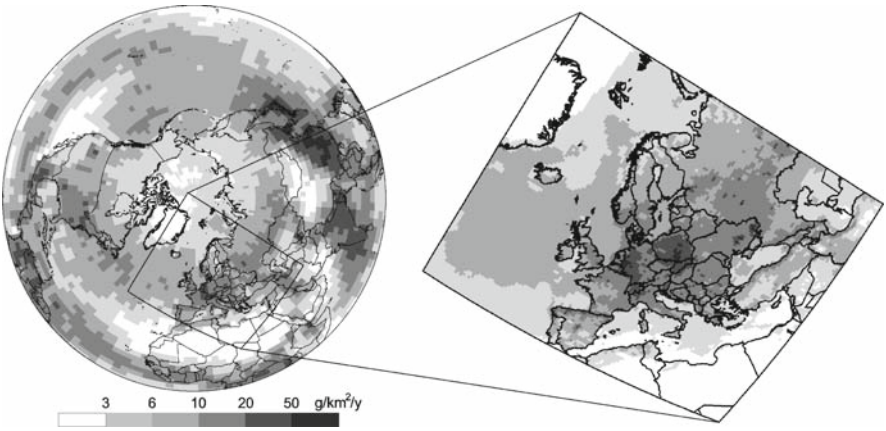

Figure 20.3 Spatial distribution of total mercury deposition in the Northern Hemisphere and in Europe in 2001

In general, spatial distribution of deposition well corresponds to the emission field (Figure 20.2b): Elevated deposition fluxes (more than 20 g km^{-2} yr^{-1}) were in Europe, North America, Eastern and Southern Asia. Mercury deposition in these regions are defined to a greater extent by primary short-lived mercury forms (oxidized gaseous and particulate mercury) directly emitted to the atmosphere from local anthropogenic sources. On the other hand, deposition over remote regions depend on *in situ* oxidation of elemental mercury transported from various continents.

Therefore, considerable deposition fluxes over some parts of the Atlantic and Pacific oceans (up to 12 g km^{-2} yr^{-1}) are result of combination of two factors: relatively high concentrations of the oxidants (tropospheric ozone first of all) and elevated precipitation amount in these regions. Here we consider only long-term deposition of mercury to the surface and do not take into account its fast circulation between air and seawater in the marine boundary layer (e.g. Laurier et al., 2003; Hedgecock and Pirrone, 2004). The lowest deposition fluxes were predicted over desert regions in Africa and in some areas of the Arctic mostly because of small precipitation amount. However, it should be noted that chemical mechanism of mercury depletion events (MDEs) was not taken into account in this study. Thus, one can expect that mercury deposition in the Arctic is considerably higher, particularly, in the coastal areas.

Estimates of long-term changes of mercury deposition to different continents and regions of the Northern Hemisphere are presented in Figure 20.4. The most significant decrease of deposition during the considered period took place in

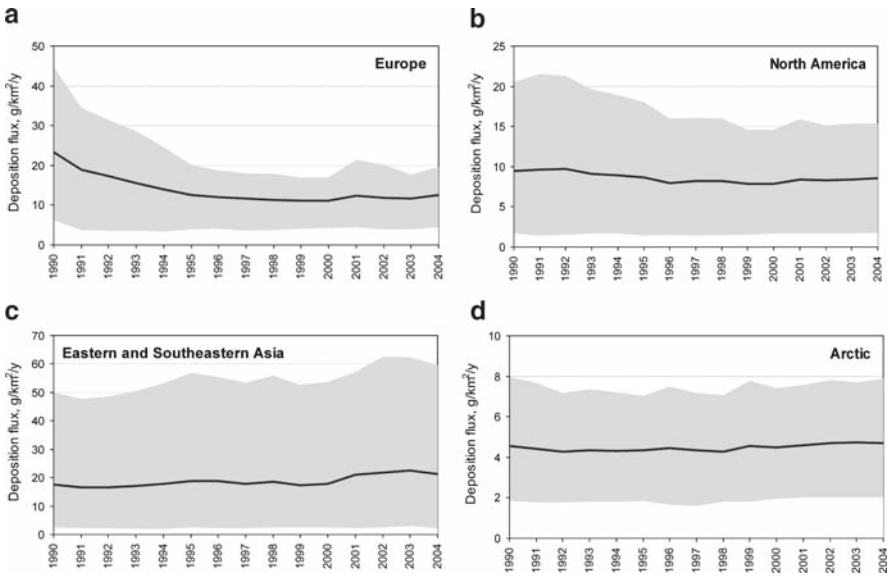

Figure 20.4 Long-term changes of mercury deposition flux in Europe (**a**), North America (**b**), Eastern and Southeastern Asia (**c**), and in the Arctic (**d**). Solid line presents average flux over the region; shaded area shows 90%-confidence interval of the flux variation over the region

Europe: the average deposition flux decreased by a factor of two, whereas the highest deposition fluxes decreased by a factor of three (Figure 20.4(a)). The reason for that is considerable emission reduction in Europe in this period (see Figure 20.2a). Changes of mercury deposition in North America (Figure 20.4(b)) are less pronounced because of smaller emission reduction and more essential contribution of mercury transport from other continents (in particular, from East Asia). In agreement with changes of anthropogenic emissions, deposition of mercury increased in Eastern and Southeastern Asia (Figure 20.4(c)). However, the increase was smoothed by decrease of emissions in other parts of the Northern Hemisphere. In the beginning of the period deposition levels in Eastern and Southeastern Asia was comparable with those in Europe and almost twice higher than in North America, whereas by the end of the period deposition in Asia became the highest in the Northern Hemisphere. Estimated mercury deposition in the Arctic did not change significantly during the 15-years period (Figure 20.4(d)) and they are several times lower than those in major industrialized continents. However, as it was mentioned above, these estimates do not take into account effect of the MDEs and, therefore, underestimate actual deposition in the Arctic. It should be also noted that some increase of mercury deposition estimated for last years of the period (2001-2004) was caused solely by changes of meteorological conditions since emissions were taken unchanged for these years.

Estimates performed by the regional version of the model with more detailed emissions for Europe (*WebDab*, 2006) demonstrate continuous decrease of deposition in Europe during the whole period including the last years (Figure 20.5(a)). In particular, Figure 20.5 shows trends of mercury deposition changes to different land use categories in Europe. As seen the largest deposition values and the most significant decrease are characteristic of urban areas. It is evident that they are located in the

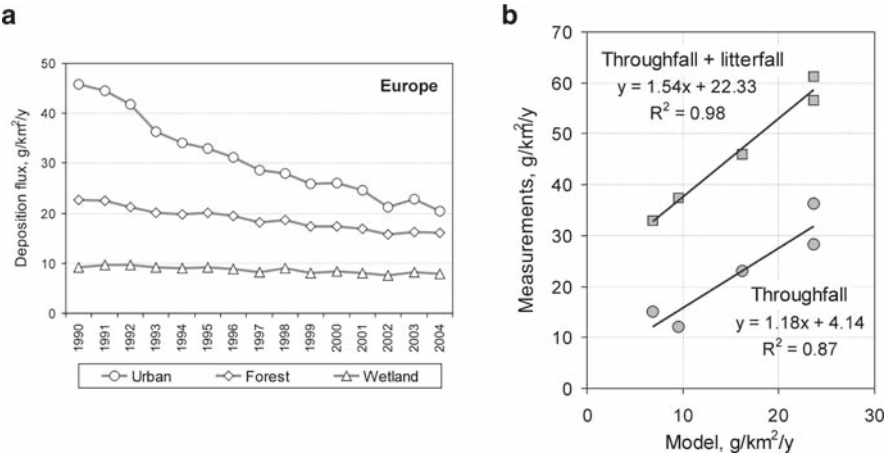

Figure 20.5 Long-term changes of mercury deposition flux to different landuse categories in Europe (**a**) and comparison of calculated mercury deposition to forests with throughfall measurements at forest sites in Europe (**b**)

immediate vicinity of main anthropogenic sources and reflect emission dynamics. On the other hand, changes of deposition to other sensitive land use categories (forest, wetland) are less pronounced because they are located more remotely from direct emission sources and more affected by transport form other continents and natural/re-emission sources. Another aspect of these estimates is connected with current understanding of mercury exchange with vegetation. Analysis of contemporary models parameterization of mercury deposition to forest reveal that simulated total (wet and dry) deposition cannot explain overall input of mercury to the forested ecosystems (Munthe, 2005). Particularly, Figure 20.5(b) presents comparison of modelled deposition fluxes with measurements at several forested ecosystems in Europe (Schwesig et al., 1999; Schwesig and Matzner, 2000; Porvari and Verta, 2003; Lee et al., 2000; Munthe et al., 1995). As seen from the figure, the model successfully reproduces throughfall deposition flux of mercury, however, it fails taking into account litterfall component of deposition, which is defined by mercury accumulated in foliage. Thus, mercury deposition simulated by the model likely significantly underestimate actual total input of mercury to forested ecosystems.

20.3.2 Evaluation of Modelling Results

In order to evaluate the modelling results calculated mercury concentrations in air and precipitation were compared with available measurements. For this purpose we used long-term observations from the EMEP monitoring network in Europe (Aas and Breivik, 2006) as well as the NADP /MDN (http://nadp.sws. uiuc.edu/mdn/) and CAMNet (Kellerhals et al., 2003) networks in North America. Besides, measurements at the Arctic stations (Barrow, Alert, Amderma), data from the MAMCS project (Pirrone et al., 2003) and some measurements from Asia (Tan et al., 2000; Kim et al., 2002) were involved in the comparison. Location of monitoring sites used in the model evaluation is shown in Figure 20.6(a). Results of the comparison of annual mean values for the period 1990-2004 are presented in Figures 20.6(b) and 20.6(c).

As seen, modelled concentrations of total gaseous mercury well agree with observed ones. Discrepancy between calculated and measured values does not exceed 20% with the exception of high values at Chinese and Korean sites which are somewhat underestimated by the model. On the other hand, the model tends to overestimate observed mercury concentration in precipitation. Besides, scattering of modelled and observed concentration in precipitation is more significant than in the case of air concentration. Nevertheless, difference between the calculated and measured values does not exceed a factor of two.

An example of comparison of measured and modelled long-term variation of mercury concentration in air and precipitation during the period 1990-2004 at some monitoring sites is shown in Figure 20.7. Both model and observations demonstrate relatively low variation of total gaseous mercury concentration in air (Figures 20.7(a) and 20.7(b)).

The model somewhat overestimate relatively low concentrations (below 1.5 ng m^{-3}) at station Pallas in Finland. Besides, it does not catch deep depressions of the concentration

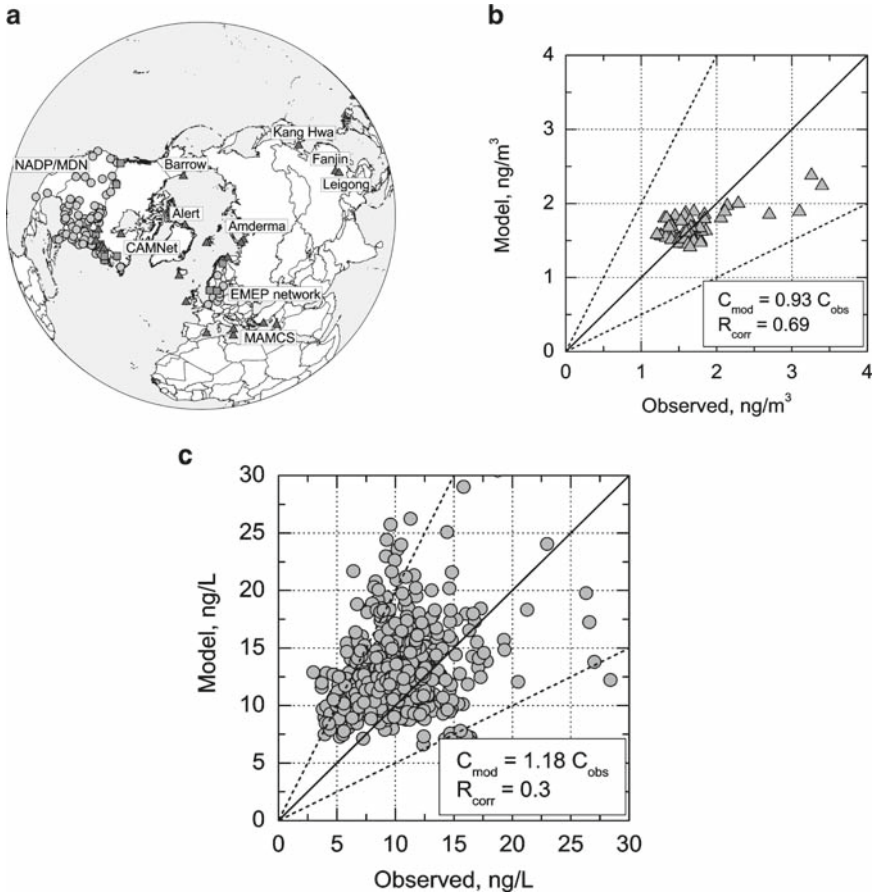

Figure 20.6 Location of monitoring sites used in the model evaluation **(a)**, calculated vs. measured values of mean annual concentration of total gaseous mercury (**b**) and mercury concentration in precipitation (**c**). Dashed lines depict two-fold difference interval

during springtime because of MDEs at the Arctic station Zeppelin located at Spitsbergen. Both measurements and the model do not show significant changes of air concentrations between 1990 and 2004. The model successfully reproduces variation of mercury concentration in precipitation (Figures 20.7(c) and 20.7(d)). The variation exhibits pronounced seasonal cycle with maximum in summer and minimum in winter, which is defined by higher concentrations of photo oxidants during summertime.

20.3.3 Intercontinental Transport

As it was demonstrated above mercury deposition in many cases is significantly affected by transport from other continents (except areas located in the immediate vicinity of direct emissions). To evaluate the influence of intercontinental transport

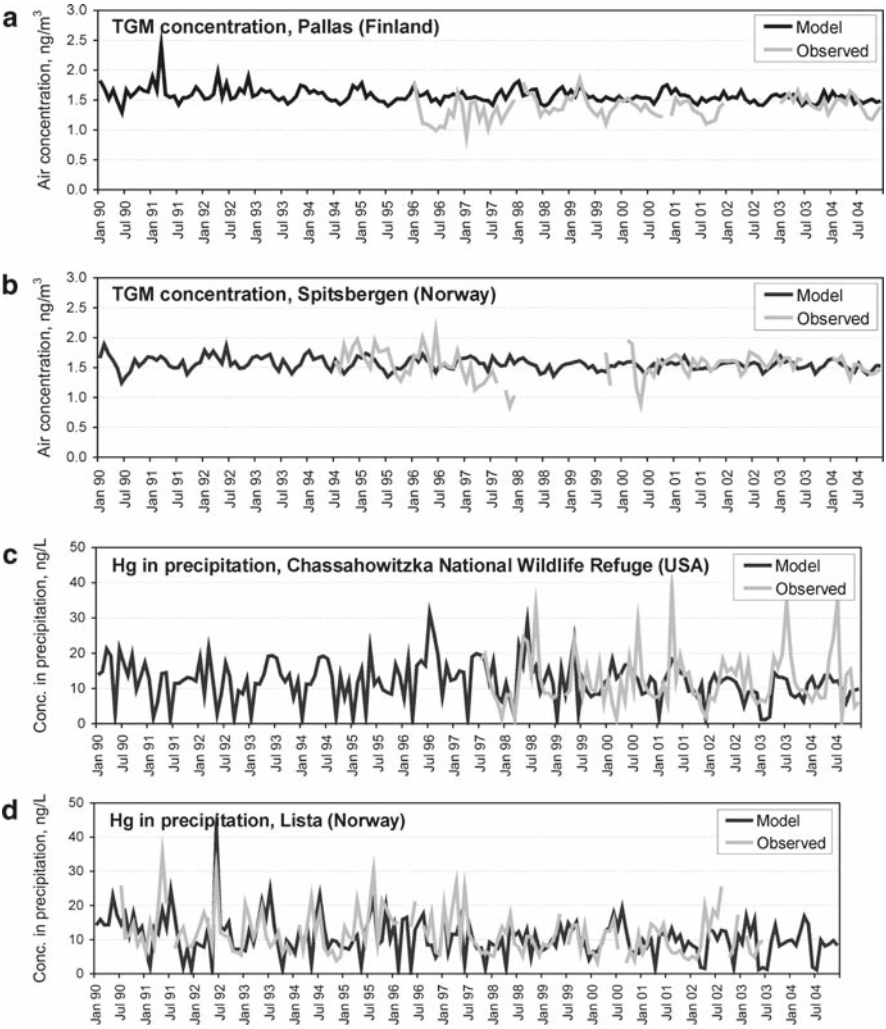

Figure 20.7 Modelled vs. measured long-term variation of monthly mean total gaseous mercury concentration in air (**a, b**) and total mercury concentration in precipitation (**c, d**) at some monitoring sites in Europe (Aas and Breivik, 2006) and North America (http://nadp.sws.uiuc.edu/mdn/)

on mercury deposition in the Northern Hemisphere and its sensitivity to emission reduction in different continents we performed model runs with anthropogenic emissions decreased by 20% in four major source regions – Europe, North America, East Asia and South Asia (see Figure 20.2 (b)) – with respect to the base case for the year 2001.

Figure 20.8 illustrates spatial patterns of simulated decrease mercury deposition in the Northern Hemisphere due to 20% emission reduction in the mentioned above regions. Mercury deposition in the Northern Hemisphere are the most sensitive to emission reduction in East Asia (Figure 20.8(a)) because of large relative contribution

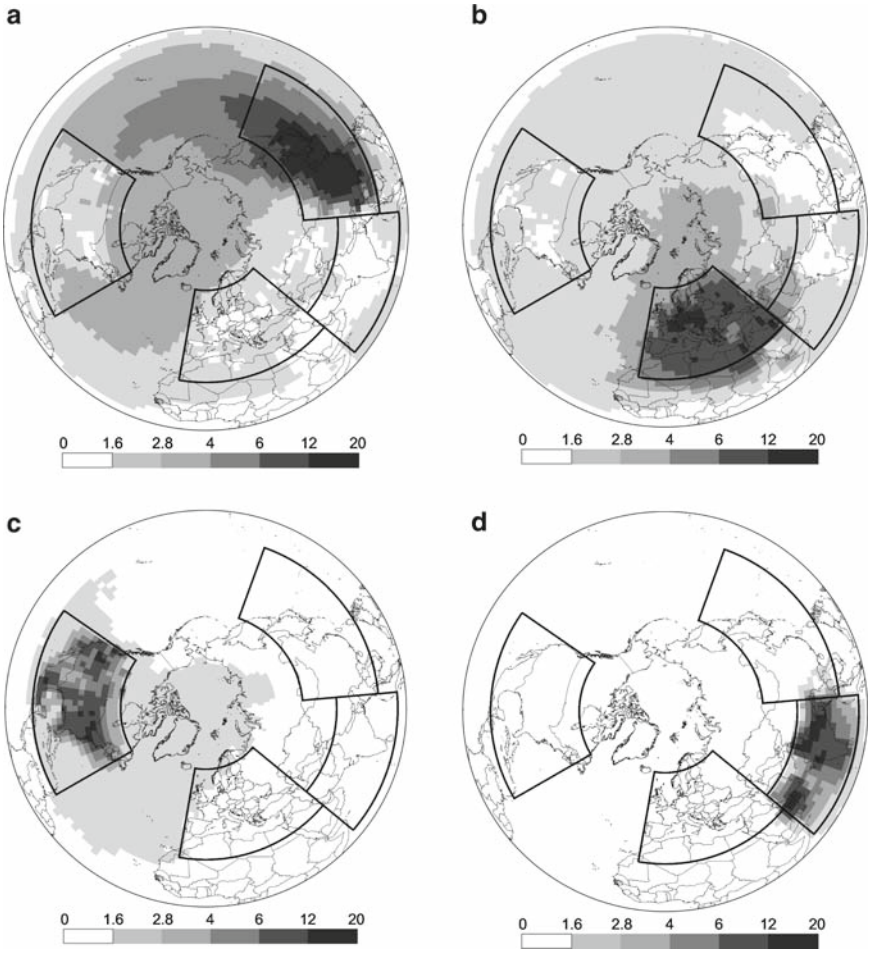

Figure 20.8 Spatial distribution of relative decrease of mercury deposition due to 20% emission reduction in East Asia (**a**), Europe (**b**), North America (**c**), and South Asia (**d**)

of sources located in this region to the global mercury emissions. Deposition of mercury decreases considerably not only in Eastern Asia but also over the North Pacific, North America and the Arctic. Emission reduction in Europe also results in considerable deposition decrease (apart from in Europe itself) in the North Atlantic, the Arctic and Northern Africa (Figure 20.8(b)). Decrease of mercury emissions in North America partly affects deposition in the North Atlantic and the Arctic (Figure 20.8(c)). Emission reduction in Southern Asia has the lowest effect on decrease of mercury deposition in the Northern Hemisphere (Figure 20.8(d)). The probability distribution of the deposition decrease values over the Northern Hemisphere with respect to 20% emission reduction in four selected regions is characterized quantitatively in Figure 20.9(a). As seen from the figure the most probable values of the

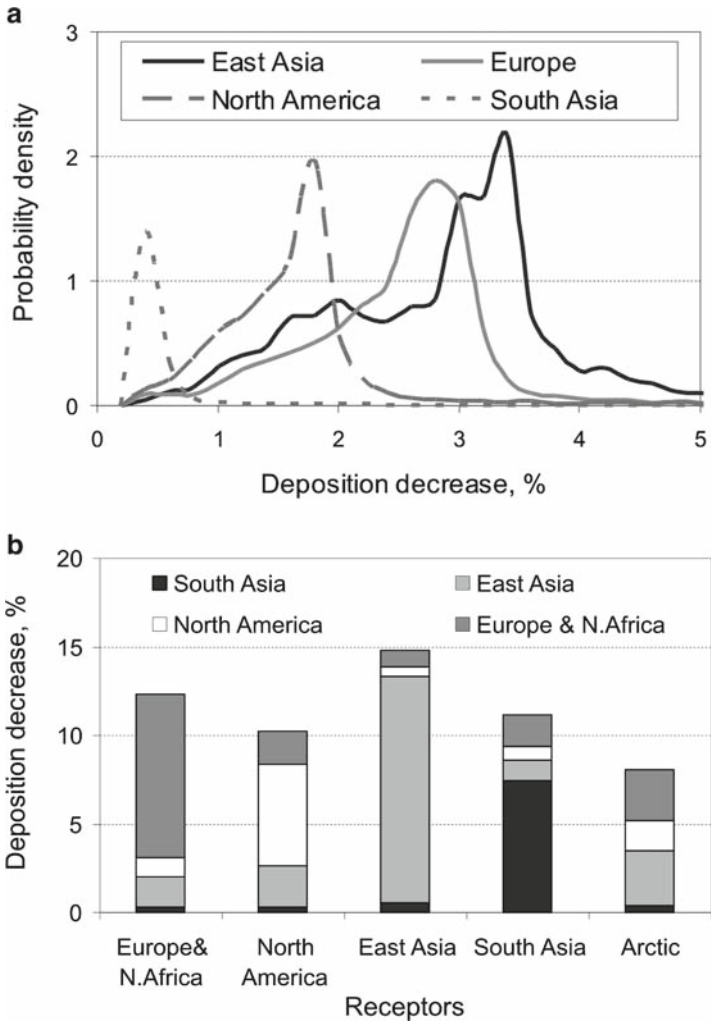

Figure 20.9 Probability distribution of mercury deposition decrease over the Northern Hemisphere due to 20% emission reduction in the selected source regions (**a**) and contribution of the source regions to the deposition decrease in different receptor regions (**b**)

deposition decrease are 3.2%, 2.8%, 1.8%, and 0.4% for East Asia, Europe, North America and South Asia, respectively.

The relative contribution of different source regions to the deposition reduction of mercury over various receptor regions is illustrated in Figure 20.9(b). As seen deposition in Europe is most sensitive to reduction of anthropogenic emissions from its own sources but also in Eastern Asia and North America. Deposition decrease in East and South Asia is also mostly defined by reduction of emissions from own sources. On the other hand, mercury deposition in North America only

partly depends on emissions from own sources but also to a great extent on those from East Asian and European sources. Deposition to the Arctic are almost equally sensitive to changes of emissions in East Asia and in Europe and also partly to those in North America. Total deposition decrease due to 20% emission reduction in all four regions varies from 8% in the Arctic to 15% in East Asia.

20.4 Uncertainty and Future Research

The analysis presented above analysis contains significant uncertainties. First of all, one of the most essential input data for mercury atmospheric dispersion modelling – anthropogenic emissions – remain incomplete and rather uncertain. The most resent global estimates of anthropogenic emissions relate to the year 2000 (Pacyna et al., 2006) and do not include some important parameters such as temporal variation of emissions. Therefore, further development of mercury atmospheric modelling requires update and improvement of global emissions data. Another important information affecting quality of mercury modelling is data on natural emission and re-emission of mercury. According to available estimates (Mason and Sheu, 2002; Strode et al., 2007) mercury evasion from land and the ocean significantly contributes to total mercury emission to the atmosphere and even likely exceeds the anthropogenic one. Therefore, reliable spatially and temporally resolved data on natural emission and re-emission are critical for estimates of realistic mercury deposition levels. A possible solution of this problem is development of a global multi-media modelling system taking into account mercury cycling in the environment and its accumulation in different environmental compartments. Among the most uncertain model processes one could select atmospheric chemistry and dry deposition (particularly, to vegetation). Additional studies are needed to refine chemical constants of the most important oxidation reactions with ozone, hydroxyl radical, halogens and improvement of model parameterisation of dry deposition of different mercury species. Available long-term measurement data do not allow complete evaluation of modelled mercury concentration and deposition levels because they are mostly located in North America and Europe. There are large territories in Africa and Asia not covered by observations at all and only episodic measurements are available from the oceans. Besides, very scarce measurement data is available on mercury dry deposition and speciated air concentrations. Development of a global monitoring network of long-term observation including measurements of different mercury species could significantly improve evaluation of modelling results.

References

Andersson, M., Wängberg, I., Gårdfeldt, K., Munthe, J., 2004. Investigation of the Henry's low coefficient for elemental mercury. Proceedings of the 7th Conference "Mercury as a global pollutant". RMZ – Materials and Geoenvironment, Ljubljana, June 2004

Aas W. and Breivik K., 2006. Heavy metals and POP measurements, 2004. EMEP/CCC-Report 7/2006, Kjeller, Norwegian Institute for Air Research, Oslo. (www.nilu.no/ projects/ccc/ reports.html)

Ariya P.A., Khalizov A., Gidas A. (2002) Reactions of gaseous mercury with atomic and molecular halogens: kinetics, product studies, and atmospheric implications. *J. Phys. Chem.* 106, 7310–7320

Behrenfeld M.J. and Falkowski P.G. (1997) Photosynthetic derived from satellite-based chlorophyll concentration. *Limnol. Oceanogr.*, 42(1), 1–20

Carpi A. and Lindberg S. E. (1998) Application of a teflonTM dynamic flux chamber for quantifying soil mercury flux: tests and results over background soil. *Atmos. Environ.* 32(5), 873–882

CGEIC website, http://www.ortech.ca/cgeic/

Chin M., Jacob D.J., Gardner G.M., Forman-Fowler M.S., Spiro P.A., Savoie D.L. (1996) A global three-dimensional model of tropospheric sulfate, *J. Geophys. Res.* 101, 18667–18690

Gårdfeldt K., Sommar J., Strömberg D., Feng X. (2001) Oxidation of atomic mercury by hydroxyl radicals and photoinduced decomposition of methylmercury in the aqueous phase. *Atmos. Environ*. 35, 3039–3047

Grell GA, Dudhia J, and Stauffer DR. (1995) A description of the Fifth-Generation Penn State / NCAR Mesoscale Model (MM5). NCAR Technical Note NCAR/TN-398+STR. Mesoscale and Microscale Meteorology Division, National Center for Atmospheric Research, Boulder, Colorado, 122 pp.

Gustin M.S., Lindberg S., Marsik F., Casimir A., Ebinghaus R., Edwards G., Hubble-Fitzgerald C., Kemp R., Kock H., Leonard T., London J., Majewski M., Montecinos C., Owens J., Pilote M., Poissant L., Rasmussen P., Schaedlich F., Schneeberger D., Schroeder W., Sommar J., Turner R., Vette A., Wallschlaeger D., Xiao Z., and Zhang H. (1999) Nevada STORMS project: Measurement of mercury emissions from naturally enriched surfaces. *J. Geophys. Res.* 104(D17), 21831–21844

Hall B. (1995) The gas phase oxidation of mercury by ozone. *WASP* 80, 301–315

Jacobson, M. Z., 1999. Fundamentals of atmospheric modeling. Cambridge University Press. 656 p.

Hedgecock I.M., Pirrone N. (2004) Chasing Quicksilver: Modelling the Atmospheric Lifetime of $Hg^0_{(g)}$ in the marine boundary layer at various latitudes. *Environ. Sci. Technol*. 38, 69–76

Kellerhals M., Beauchamp S., Belzer W., Blanchard P., Froude F., Harvey B., McDonald K., Pilote M., Poissant L., Puckett K., Schroeder B., Steffen A., Tordon R. (2003) Temporal and spatial variability of total gaseous mercury in Canada: results from the Canadian Atmospheric Mercury Measurement Network (CAMNet). *Atmos. Environ*. 37(7), 1003–1011

Kim K.-H., Lindberg S. E. and Meyers T. P. (1995) Micrometeorological measurements of mercury vapor fluxes over background forest souls in eastern Tennessee. *Atmos. Environ.* 29(2), 267–282

Kim, K.-H., Kim, M.-Y., Kim, J., Lee, G. (2002) The concentrations and fluxes of total gaseous mercury in a western coastal area of Korea during late Mart 2001. *Atmos. Environ.* 36, 3413–3427

Lamborg C.H., Fitzgerald W.F., O'Donnell J., Torgersen T. (2002) A non-steady state compartmental model of global-scale mercury biogeochemistry with interhemispheric atmospheric gradients. *Geochim. Cosmochim. Acta* 66, 1105–1118

Laurier F.J.G., Mason R.P., Whalin L., Kato S. (2003) Reactive gaseous mercury formation in the North Pacific Ocean's marine boundary layer: A potential role of halogen chemistry. *J. Geophys. Res.* 108(D17), 4529

Lee Y.H., Bishop K.H., Munthe J. (2000) Do concepts about catchment cycling of methylmercury and mercury in boreal catchments stand the test of time? Six years of atmospheric inputs and runoff export at Svartberget, northern Sweden. *Sci. Tot. Environ*. 249, 11–20

Lin C.-J., Pehkonen S. O. (1999) The chemistry of atmospheric mercury: a review. *Atmos. Environ.* 33, 2067–2079

Lurie Yu. Yu. [1971] Handbook for Analytical Chemistry. Khimiya, Moscow, 454 p.

Mason R.P. and Sheu G.-R. (2002) Role of the ocean in the global mercury cycle. *Glob. Biogeochem. Cycles* 16(4), 1093, doi:10.1029/2001GB001440

Munthe J. (1992) The aqueous oxidation of elemental mercury by ozone. *Atmos. Environ.* 26A, 1461–1468

Munthe J., Hultberg H., Iverfeldt Å. (1995) Mechanisms of deposition of methylmercury and mercury to coniferous forests. *WASP* 80, 363–371

Munthe (2005) personal communication

Pacyna J, Pacyna E, Steenhuisen F, Wilson S. (2003) Mapping 1995 global anthropogenic emissions of mercury. *Atmos. Environ.* 37(S1), S109–S117

Pacyna E. G., Pacyna J. M., Steenhuisen F. and Wilson S. (2006) Global anthropogenic mercury emission inventory for 2000. *Atmos. Environ.* 40(22), 4048–4063

Pirrone N., Ferrara R., Hedgecock I. M., Kallos G., Mamane Y., Munthe J., Pacyna J. M., Pytharoulis I., Sprovieri F., Voudouri A., Wangberg I. (2003) Dynamic Processes of Mercury Over the Mediterranean Region: results from the Mediterranean Atmospheric Mercury Cycle System (MAMCS) project. *Atmos. Environ.* 37(S1), 21–39

Petersen G., Munthe J., Pleijel K., Bloxam R., Vinod Kumar A. (1998) A comprehensive Eulerian modeling framework for airborne mercury species: development and testing of the tropospheric chemistry module (TCM). *Atmos. Environ*. 32, 829–843

Poissant L. and Casimir A. (1998) Water–air and soil–air exchange rate of total gaseous mercury measured at background sites. *Atmos. Environ*. 32(5), 883–893

Porvari, P., Verta, M. (2003) Total and methyl mercury concentrations and fluxes from small boreal forest catchments in Finland. *Environ. Pollut.* 123(2), 181–191

Rubinstein K., Kiktev D. (2000) Comparison of the atmospheric low-layer diagnostic system (SDA) for pollution transfer modelling at MSC-East (Moscow) and MSC-West (Oslo). *Environmental Modelling & Software* 15, 589–596

Ruijgrok W., Tieben H., Eisinga P. (1997) The dry deposition of particles to a forest canopy: a comparison of model and experimental results. *Atmos. Environ.* 31, 399 – 415

Ryaboshapko A., Ilyin I., Bullock R., Ebinghaus R., Lohman K., Munthe J., Petersen G., Segneur C., Wangberg I. (2001) Intercomparison study of numerical models for long-range atmospheric transport of mercury. Stage I: Comparison of chemical modules for mercury transformations in a cloud/fog environment. EMEP/MSC-E Technical report 2/2001, Meteorological Synthesizing Centre – East, Moscow, Russia (www.msceast.org/publications.html)

Sander R. (1997) Henry's law constants available on the Web. EUROTRAC Newsletter 18, 24-25 (www.mpch-mainz.mpg.de/~sander/res/henry)

Schwesig D., Ilgen G., Matzner E. (1999) Mercury and methylmercury in upland and wetland acid forest soils of a watershed in NE-Bavaria, Germany. *WASP* 113, 141–154.

Schwesig D., and Matzner E. (2000) Pools and fluxes of mercury and methylmercury in two forested catchments in Germany. *Sci. Total Environ*. 260, 213–223

Seigneur C., Karamchandani P., Lohman K., Vijayaraghavan K., Shia R.-L., 2001. Multiscale modeling of the atmospheric fate and transport of mercury. *J. Geophys. Res.* 106, 27795–27809

Slemr F. (1996) Trends in atmospheric mercury concentrations over the Atlantic ocean and the Wank Summit, and the resulting concentrations on the budget of atmospheric mercury. In: Baeyens W., Ebinghaus R. Vasiliev O. (Eds.), Global and Regional Mercury Cycles: Sources, Flaxes and Mass Balances, pp. 33–84. NATO-ASI-Series, Kluwer Academic Publishers, Dordrecht, The Netherlands.

Slinn W.G.N. (1982) Predictions for particle deposition to vegetative canopies. *Atmos. Environ*. 16, 1785–1794

Spivakovsky C.M., Logan J.A., Montzka S.A., Balkanski Y.J., Foreman-Fowler M., Jones D.B.A., Horowitz L.W., Fusco A.C., Brenninkmeijer C.A.M., Prather M.J., Wofsy S.C., McElroy M.B. (2000) Three-dimensional climatological distribution of tropospheric OH: Update and evaluation. *J. Geophys. Res*. 105, 8931–8980

Sommar J., Gårdfeldt K., Strömberg D., Feng X. (2001) A kinetic study of the gas-phase reaction between the hydroxyl radical and atomic mercury. *Atmos. Environ*. 35, 3049–3054

Strode S.A., Jaegle L., Selin N., Jacob D.J., Park R.J., Yantosca R.M., Mason R.P., Slemr F. (2007) Air-sea exchange in the global mercury cycle. *Glob. Biogeochem. Cycles* 21(4), GB1017

Tan H., He J.L., Liang L., Lazoff S., Sommer J., Xiao Z.F., Lindqvist O. (2000) Atmospheric mercury deposition in Guizhou, China. *Sci. Total Environ*. 259, 223–230

Travnikov O, Ryaboshapko A. (2002) Modelling of mercury hemispheric transport and depositions. EMEP/MSC-E Technical Report 6/2002, Meteorological Synthesizing Centre - East, Moscow, Russia. (www.msceast.org/publications.html)

Travnikov O, Ilyin I. (2005) Regional model MSCE-HM of heavy metal transboundary air pollution in Europe. EMEP/MSC-E Technical Report 6/2005, Meteorological Synthesizing Centre - East, Moscow, Russia. (www.msceast.org/publications.html)

Travnikov O. (2005) Contribution of the intercontinental atmospheric transport to mercury pollution in the Northern Hemisphere. *Atmos. Environ*. 39, 7541–7548

Walton J.J., MacCracken M.C. and Ghan S.J. (1988) A global-scale Lagrangian trace species model of transport, transformation, and removal processes. *J. Geophys. Res*. 93(D7), 8339–8354

Wang N., Logan J.A., Jacob D.J. (1998) Global simulation o ftropospheric O3-Nox-hydrocarbon chemistry, 2., Model evaluation and global ozone budget. *J. Geophys. Res*. 103, 10727–10755

WebDab (2006), http://webdab.emep.int/

Wesely M.L., Cook D.R., Hart R.L. (1985) Measurements and parameterization of particulate sulfur dry deposition over grass. *J. Geophys. Res.* 90, 2131–214

Wesely M.L. and Hicks B.B. (2000) A review of the current status of knowledge on dry deposition. *Atmos. Environ*. 34, 2261–22

Williams R.M. (1982) A model for the dry deposition of particles to natural water surfaces. *Atmos. Environ*. 16, 1933–1938

Zhang H., Lindberg S. E., Marsik F. J., and Keeler G. J. (2001) Mercury air/surface exchange kinetics of background soils of the Tahquamenon River watershed in the Michigan upper peninsula. *WASP* 126, 151–169